Article

Design, Synthesis, and Biological Evaluation of Tetrazole Analogs of Cl-Amidine as Protein Arginine Deiminase Inhibitors

Venkataraman Subramanian,[†] Jason S. Knight,[‡] Sangram Parelkar,[†] Lynne Anguish,[§] Scott A. Coonrod,[§] Mariana J. Kaplan,[∥] and Paul R. Thompson*,[†]

[†]Department of Biochemistry and Molecular Pharmacology, University of Massachusetts Medical School, 364 Plantation Street, Worcester, Massachusetts, 01605, United States

[‡]Division of Rheumatology, University of Michigan Medical School, 1150 W. Medical Center Drive, Ann Arbor, Michigan 48109, United States

[§]Department of Molecular Biology and Genetics, Baker Institute for Animal Health, College of Veterinary Medicine, Cornell University, Hungerford Hill Road, Ithaca, New York 14853, United States

[∥]National Institute of Arthritis and Musculoskeletal and Skin Diseases (NIAMS), 10 Center Drive, MSC 1560, Bethesda, Maryland 20892, United States

S *Supporting Information*
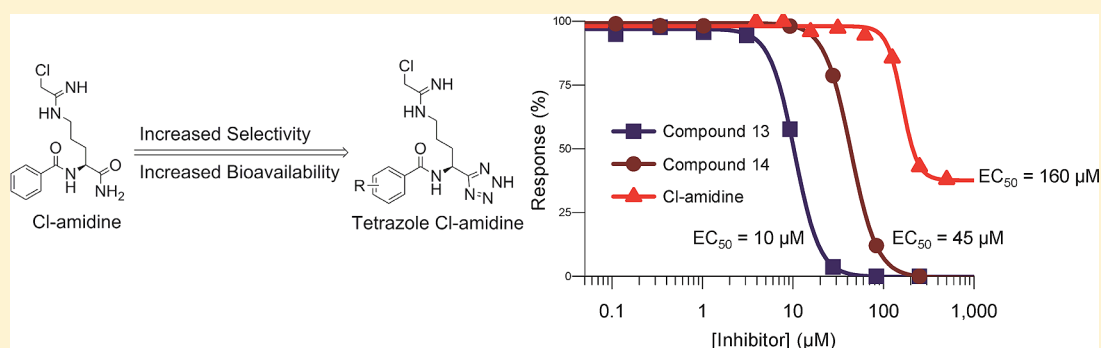
ABSTRACT: Protein arginine deiminases (PADs) catalyze the post-translational hydrolysis of arginine residues to form citrulline. This once obscure modification is now known to play a key role in the etiology of multiple autoimmune diseases (e.g., rheumatoid arthritis, multiple sclerosis, lupus, and ulcerative colitis) and in some forms of cancer. Among the five human PADs (PAD1, -2, -3, -4, and -6), it is unclear which isozyme contributes to disease pathogenesis. Toward the identification of potent, selective, and bioavailable PAD inhibitors that can be used to elucidate the specific roles of each isozyme, we describe tetrazole analogs as suitable backbone amide bond bioisosteres for the parent pan PAD inhibitor Cl-amidine. These tetrazole based analogs are highly potent and show selectivity toward particular isozymes. Importantly, one of the compounds, biphenyl tetrazole *tert*-butyl Cl-amidine (compound **13**), exhibits enhanced cell killing in a PAD4 expressing osteosarcoma bone marrow (U2OS) cell line and can also block the formation of neutrophil extracellular traps. These bioisosteres represent an important step in our efforts to develop stable, bioavailable, and selective inhibitors for the PADs.

■ INTRODUCTION

Protein arginine deiminases (PADs), members of the amidinotransferase superfamily of enzymes, catalyze the hydrolysis of arginine residues to form citrulline (Figure 1).[1−3] There are five PADs (PAD1, -2, -3, -4, and -6) in humans and other mammals.[1−3] These enzymes are highly related with 50% interisozyme sequence identity and require micromolar levels of calcium for full activity; calcium binding causes a conformational change that allosterically activates the enzymes.[1−3] Although highly related, these enzymes display unique tissue distribution patterns. For example, PAD2 is expressed in most tissues and cell types, whereas PAD1 and PAD3 are generally restricted to the skin and hair follicles and PAD4 and PAD6 are primarily expressed in neutrophils and
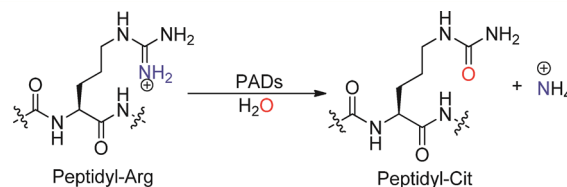

Figure 1. Protein arginine deiminases (PADs) convert arginine residues into citrulline.

oocytes, respectively.[3] Although we are only beginning to understand how the PADs contribute to normal human physiology, it is known that these enzymes help control myelination, differentiation, the epigenetic control of gene transcription, the innate immune response, and the maintenance of pluripotency.[4,5] In addition to these processes, dysregulated PAD activity is associated with the onset and progression of multiple inflammatory diseases (e.g., rheumatoid arthritis, multiple sclerosis, lupus, inflammatory bowel disease, and ulcerative colitis) and also some forms of cancer.[3,6–14]

Although it is not understood how the PADs contribute to such a disparate number of diseases, common links include their role in controlling the formation of neutrophil extracellular traps (NETs) as well as their ability to modulate the expression of both proliferative and antiproliferative genes.[15,16] The overwhelming evidence linking dysregulated PAD activity to disease pathogenesis prompted the initiation of several PAD inhibitor programs.[17,18] Prior work in this area includes the identification of several reversible PAD inhibitors (e.g., Taxol, methylarginines, and minocycline); however, these compounds are very weak PAD inhibitors or have multiple off targets.[19–27] As such, they have shown limited utility as tool compounds to study PAD biology. By contrast, the haloacetamidine class of compounds has provided key insights into PAD biology.[17,18] Cl-amidine, the most widely used member of this compound class, has been used to demonstrate PAD involvement in the maintenance of pluripotency, the epigenetic control of gene transcription, and the formation of neutrophil extracellular traps.[16,28–32] Additionally, Cl-amidine shows efficacy in multiple preclinical models of autoimmunity and cancer including ulcerative colitis, lupus, rheumatoid arthritis, and atherosclerosis as well as breast cancer.[12,33–41] To enhance the potency, selectivity, and bioavailability of Cl-amidine, we and others have generated a number of derivatives including TDFA (a tripeptide F-amidine analog) and YW3-56.[12,42] However, these compounds are all peptide based and subject to degradation by proteolysis. This is even the case for Cl-amidine (Scheme 1) because the basic chemical scaffold (i.e., benzoyl arginine amide, BAA) is a trypsin substrate.

Scheme 1. C-Terminal Bioisosteric Modification of Cl-amidine
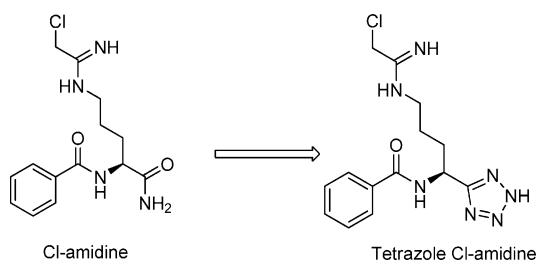
Recently, we synthesized a series of D-ornithine based compounds hypothesizing that these analogs would be more stable relative to their L-amino acid counterparts.[43] Although subsets were potent PAD inhibitors, D-amino acid derivatives showed only minor improvements in their overall stability. In our continuous efforts to identify stable, potent, and selective inhibitors for the PADs, we describe herein, the design, synthesis, and biological evaluation of tetrazole analogs of Cl-amidine.
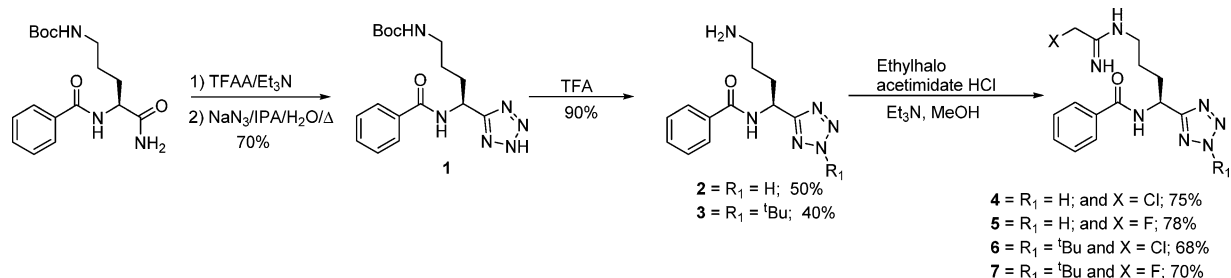
RESULTS AND DISCUSSION

Chemistry. Given that tetrazoles are bioisosteres for carboxylic acids and cis/trans amides,[44–46] we hypothesized that the replacement of the C-terminal amide bond in Cl-amidine with a tetrazole ring would improve the stability of the parent compound. Notably, the tetrazolium ring tends to be ionized at pH 7.4, exhibiting a pK_a value of 4.9, thereby mimicking the electronegativity of the C-terminal carboxamide. The synthesis of these tetrazole based analogs began with the corresponding Bz-Orn(Boc)-amide (Scheme 2). The C-terminal carboxamide was dehydrated with triethylamine and TFAA to give the corresponding cyano compound. The cyano ornithine was then heated with sodium azide in $^iPrOH/H_2O$ to generate the tetrazole. Deprotection of the Boc protecting group with TFA led to the formation of two products in one pot: the desired tetrazole and a tetrazole tert-butyl derivative. The attachment of a tert-butyl group onto a highly acidic tetrazolium ring during the course of Boc cleavage with TFA has precedence in the literature.[47] Note that these substituted tetrazoles are no longer acidic because of substitution of the acidic nitrogen. The tetrazole and tetrazole tert-butyl derived ornithines were separated by HPLC, and then the chloro- and fluoroacetamidine warheads were installed using standard protocols.[48] Purification yielded a series of tetrazole derived haloacetamidines in good yield (68–78%) (Scheme 2).

With the tetrazole chemistry in place, we next considered that replacement of the N-terminal benzoyl group with a biphenyl benzoyl moiety would increase the hydrophobicity of the compound to enhance cellular uptake. To this end, the commercially available H_2N-Orn(Boc)-OH was treated with 4-phenylbenzoyl chloride to give biphenyl benzoyl ornithine which was converted to the corresponding amide. The amide was then further converted to the corresponding tetrazole and tetrazole tert-butyl ornithine derivatives using the methodology outlined in Scheme 3. The warheads were then attached to the individual ornithine to give another set of compounds in good yield (>68%).

Since o-Cl-amidine and o-F-amidine are highly potent PAD inhibitors,[35] we anticipated that the attachment of an o-carboxylate on the phenyl group at the N-terminus of the tetrazole based compounds would also enhance compound potency and selectivity for the PAD isozymes. The synthesis of o-carboxylates began with Fmoc-Orn(Boc)-amide which was converted to the corresponding tetrazole compound in two steps (Scheme 4). The Fmoc group was then cleaved with 20% piperidine in DMF, and the resulting compound was treated with phthalic anhydride in THF at room temperature to install the o-carboxylate on the phenyl ring. The Boc group was then cleaved with TFA, which afforded the tetrazole and tetrazole tert-butyl ornithines in good yield. The chloro- and fluoroacetamidine warheads were then installed to give the desired o-carboxylate tetrazole derivatives (Scheme 4).

Compound Potency and Selectivity. With the tetrazole analogs in hand (4–7, 11–14, 19–22), we next evaluated their potency and selectivity by determining k_{inact}/K_I values for PAD1, -2, -3, and -4. k_{inact}/K_I is used because it is the best measure of potency for an irreversible inhibitor. PAD6 was not tested because it shows no in vitro activity. Notably, the highest potencies and selectivities were obtained for the o-carboxyl-containing tetrazoles (Figure 2, Table S1). We have previously reported that the installment of a carboxyl group ortho to the N-terminal amide increases potency,[35] likely because of the

Scheme 2. Synthesis of Tetrazole Analogs of Cl-amidine and F-amidine

2 = R₁ = H; 50%
3 = R₁ = ᵗBu; 40%

4 = R₁ = H; and X = Cl; 75%
5 = R₁ = H; and X = F; 78%
6 = R₁ = ᵗBu and X = Cl; 68%
7 = R₁ = ᵗBu and X = F; 70%

Scheme 3. Synthesis of Biphenyl Tetrazole Analogs of Cl-amidine and F-amidine

8 = R = Ph; 80%

9 = R = Ph; R₁ = H; 52%
10 = R = Ph; R₁ = ᵗBu; 37%

11 = R = Ph; R₁ = H and X = Cl; 75%
12 = R = Ph; R₁ = H and X = F; 70%
13 = R = Ph; R₁ = ᵗBu and X = Cl; 75%
14 = R = Ph; R₁ = ᵗBu and X = F; 68%
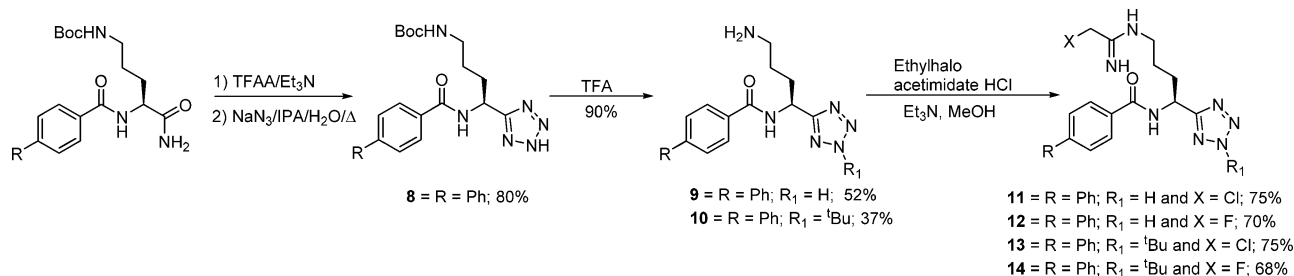
Scheme 4. Synthesis of *o*-Carboxylate Containing Tetrazole Analogs of Cl-amidine and F-amidine

17 = R₁ = H
18 = R₁ = ᵗBu

19 = R₁ = H and X = Cl; 60%
20 = R₁ = H and X = F; 61%
21 = R₁ = ᵗBu and X = Cl; 55%
22 = R₁ = ᵗBu and X = F; 52%
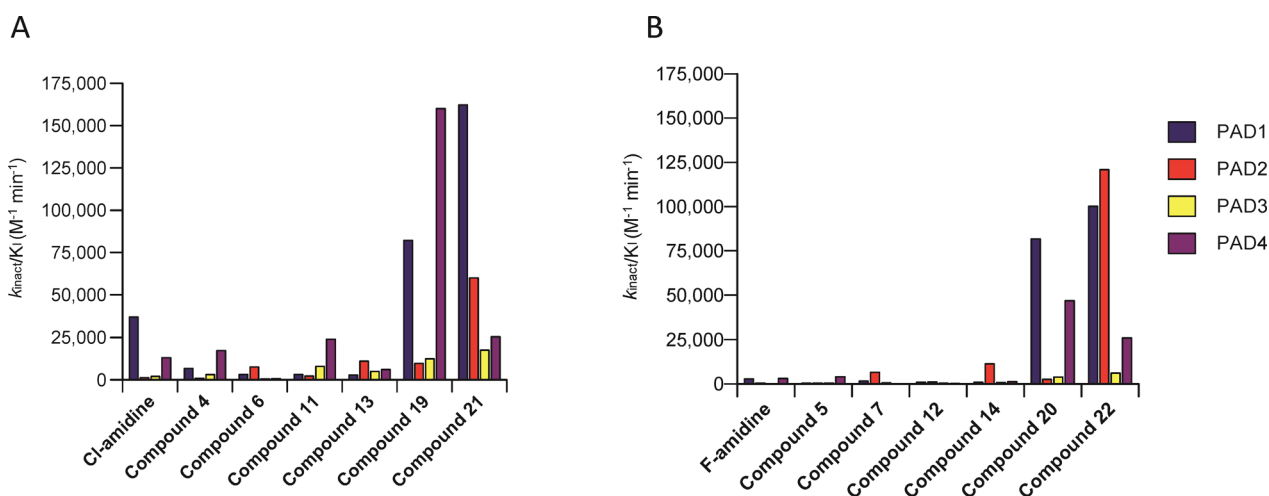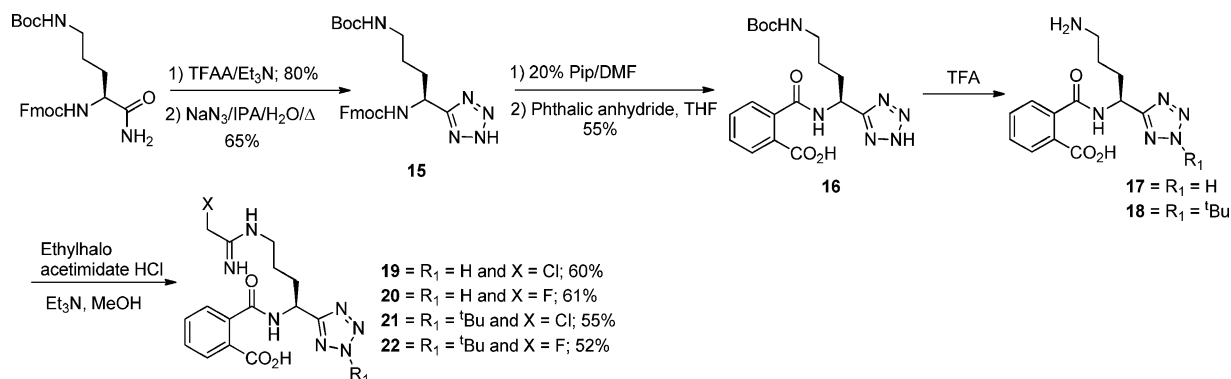
Figure 2. Selectivity of tetrazole haloacetamidines: (A) selectivity of tetrazole analogs of Cl-amidine; (B) selectivity of tetrazole analogs of F-amidine.

formation of favorable H-bonding and/or electrostatic interactions between the *o*-carboxylate and W347 and R374.[35] For Cl-ortho tetrazole (**19**), the k_{inact}/K_I values are 82 000 and 159 000 M^{-1} min^{-1} for PAD1 and PAD4, respectively. Cl-ortho

tetrazole (**19**) also showed 15-fold selectivity versus PAD2 and PAD3. F-ortho tetrazole (**20**) was similarly potent for PAD1 and exhibits 20- to 30-fold selectivity over PAD2 and PAD3 when compared to PAD1. Interestingly, the use of the
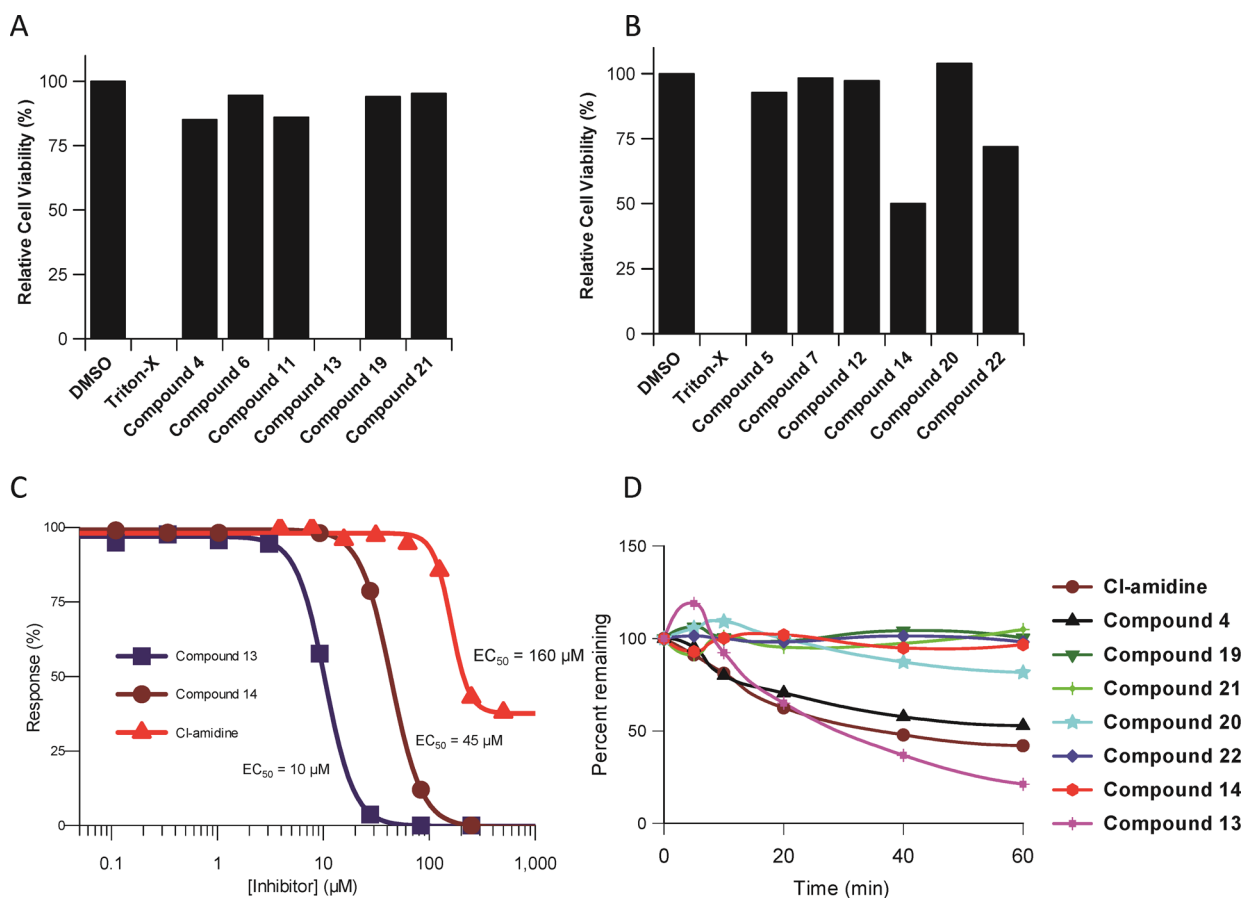
Figure 3. Cell efficacy studies. (A) Cell viability studies with the tetrazole analogs of Cl-amidine. U2OS cells were treated with compounds at final concentration of 20 μM, and cell viability was measured by the colorimetric XTT assay. Biphenyl tetrazole *tert*-butyl Cl-amidine (**13**) completely abolishes the growth of U2OS cells at 20 μM. (B) Cell viability studies with the tetrazole analogs of F-amidine. (C) EC$_{50}$ of biphenyl tetrazole *tert*-butyl compounds. Compounds **13** and **14** have lower EC$_{50}$ values compared to Cl-amidine in U2OS cells. (D) Stability of tetrazole analogs of Cl-amidine in mouse hepatic microsomes compared to Cl-amidine.

fluoroacetamidine warhead significantly reduces the potency of this compound toward PAD4, indicating that significant selectivity can be achieved by altering the identity of the warhead. Moreover, introduction of the *tert*-butyl moiety further altered the selectivity of the remaining compounds. For example, both Cl-ortho tetrazole *tert*-butyl (**21**) and F-ortho tetrazole *tert*-butyl (**22**) show a significant improvement in their ability to inhibit PAD2. This trend was observed for the other *tert*-butyl derivatives described herein. For example, the k_{inact}/K_I values of tetrazole *tert*-butyl Cl-amidine (**6**) and tetrazole *tert*-butyl-F-amidine (**7**) for PAD2 are 7500 and 6500 M^{-1} min^{-1} versus 1200 and 380 M^{-1} min^{-1} for Cl-amidine and F-amidine, respectively. In a similar fashion, the biphenyl derived tetrazole *tert*-butyl compounds possess higher selectivity toward PAD2. For example, tetrazole *tert*-butyl-F-amidine (**7**) and biphenyl tetrazole *tert*-butyl-F-amidine (**14**) preferentially inhibit PAD2 by 3- to 25-fold with the highest selectivity being observed for PAD2 over PAD4. It is important to note that both compounds **7** and **14** are highly selective PAD2 inhibitors relative to the other PADs. The preferential inhibition of PAD2 suggests that the fluoroacetamidine warhead is more suitably oriented within the PAD2 active site. Note that since saturation was not observed in the plots of the pseudo-first-order rates of inactivation versus concentration of inhibitor, it is difficult to ascertain whether the different potencies of the compounds toward the different isozymes are

driven by effects on the reactivity of the electrophile (i.e., k_{inact}) or differences in the inherent binding affinity of the inhibitors (i.e., K_I).

Cell Viability Studies. To examine the antiproliferative activities of these tetrazole analogs, we next evaluated their ability to inhibit the growth of U2OS cells using a fixed concentration of inhibitor (i.e., 20 μM) (Figure 3A and Figure 3B). Cell viability was assessed with the colorimetric XTT assay. Impressively, biphenyl tetrazole *tert*-butyl Cl-amidine (**13**) completely abolished cell growth at 20 μM. Biphenyl tetrazole *tert*-butyl-F-amidine (**14**) also inhibited cell growth, although the effects of this compound were markedly attenuated (more than 50% of cells are viable when cells were treated with 20 μM of the fluoro analog) (Figure 3B). The remaining compounds showed no effects on cell viability at this concentration. To provide a more direct measure of the cellular potency of our two best compounds (**13** and **14**), we determined the concentration of compound that reduced cell viability by 50%, i.e., the EC$_{50}$ value (Figure 3C). Consistent with our initial screening data, the EC$_{50}$ of compound **13** (10 $\pm$ 2.5 μM) was significantly better than the value obtained for compound **14** (EC$_{50}$ = 45 $\pm$ 1.2 μM). Importantly, the EC$_{50}$ values are 16- and 3.5-fold better than those obtained for the parent compound Cl-amidine (EC$_{50}$ = 160 $\pm$ 20 μM). This improved cellular efficacy is likely due to the increased hydrophobicity of the biphenyl compound enhancing cell

penetration. Although the *o*-carboxyl containing tetrazoles are very potent in vitro PAD inhibitors, the presence of the negatively charged carboxyl group likely reduces their overall bioavailability. Overall, these data highlight the potential utility of targeting the PADs for the development of an anticancer therapeutic. This is especially true for the fluoroacetamidine containing compounds because the inherent reactivity of this warhead is quite low and shows few off targets.[49,50] We do note, however, that for the chloroacetamidine containing compounds, it is difficult to directly link their cytotoxicity to PAD inhibition versus an off target effect. We are currently using these scaffolds to develop next generation activity-based protein profiling reagents to address this possibility.

Microsomal Stability Studies. We next evaluated the stability of a subset of compounds in a murine hepatic microsome stability assay which utilizes liver microsomes. Liver microsomes possess many of the enzymes responsible for drug metabolism in vivo and are also a good predictor of drug clearance properties.[51] On the basis of these data, it is clear that the fluoroacetamidine containing compounds are significantly more stable than their chloroacetamidine containing counterparts whose half-lives are similar to that obtained for Cl-amidine (Figure 3D). The one exception is the ortho carboxyl derived tetrazole Cl-amidine (**21**) whose half-life mimics those obtained for the fluoro analogs, suggesting that modification of the N-terminus substantially improves the overall stability of the compounds.

Neutrophil Extracellular Trap (NET) Inhibition Studies. We and others have shown that PAD4 mediated histone hypercitrullination induces heterochromatin decondensation and chromatin unfolding to form NETs.[52−56] Neutrophil extracellular trap (NET) formation causes direct organ damage and can trigger endothelial and epithelial cell death.[37] Inhibition of PAD4 reduces NET formation in mouse neutrophils in vivo and human neutrophils in vitro.[15] We have also shown that Cl-amidine treatment blocks NET formation and modulates the lupus phenotype in animal models.[37] Furthermore, Cl-amidine mitigates atherosclerosis in the apolipoprotein-E $(Apoe)^{-/-}$ murine model[40] and this activity correlates with decreased NET formation. Given these precedents, we next investigated whether our two best in vitro inhibitors, i.e., compounds **13** and **21**, could block NET formation. To this end, mouse neutrophils were treated with PMA to stimulate NET formation in the absence and presence of increasing amounts of Cl-amidine, compound **13**, and compound **21**. Cl-amidine was used as the reference compound. NET formation was then quantified using the DNA/neutrophil elastase overlap assay. Though **21** is very potent in vitro, it inhibits NET formation only at very high concentrations. The negatively charged carboxyl group again likely limits its bioavailability. By contrast, the biphenyl derivative **13** is significantly more potent than Cl-amidine in the NET assays (Figure 4), despite its being a significantly poorer PAD4 inhibitor in vitro. The enhanced cellular activity likely reflects the hydrophobic nature of the compound which enhances cellular uptake. We also evaluated the toxicity of **13** and **21**, our two best inhibitors, against human neutrophils. The results of these studies indicate that **21** displays very limited cytotoxicity (EC$_{50}$ = 985 ± 20). By contrast, **13** (EC$_{50}$ = 31 ± 1.0) is considerably more toxic. Nevertheless, it is noteworthy that we see considerable inhibition of NET formation at lower doses (EC$_{50}$ ≈ 20 μM) than those that cause cell killing.
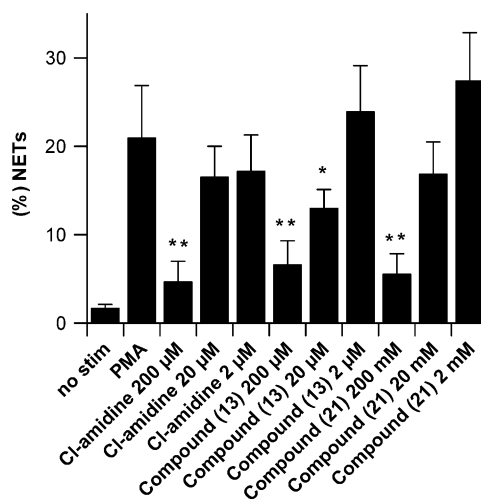

Figure 4. Biphenyl tetrazole *tert*-butyl Cl-amidine (**13**) and *o*-carboxyl tetrazole *tert*-butyl Cl-amidine (**21**) inhibit NET formation. The DNA/neutrophil elastase overlap assay suggests that compound **13** significantly reduces NET formation compared to Cl-amidine. Compound **21** also inhibits NET formation at higher doses: (∗) $p < 0.05$ and (∗∗) $p < 0.01$.

■ CONCLUSIONS

In summary, we identified tetrazoles as a suitable C-terminal bioisosteric modification of Cl-amidine. A subset of the analogs show enhanced potencies and selectivities relative to Cl-amidine. Importantly, we confirmed that installation of an *o*-carboxylate enhances the in vitro potency of the compounds by up to 30-fold highlighting the importance of this pharmacophore. We also showed that incorporation of a *tert*-butyl group on the tetrazolium ring markedly increased the selectivity of the compounds for PAD2. Finally, our data indicate that enhanced cellular permeability can be achieved by increasing the hydrophobicity of the compounds. These design characteristics will be incorporated into future analogs as part of our continuing efforts to develop isozyme specific inhibitors for all of the PADs.

■ MATERIALS AND METHODS

Chemicals. Dithiothreitol (DTT), 4-(2-hydroxyethyl)-1-piperazineethanesulfonic acid (HEPES), ammonium iron(III) sulfate dodecahydrate, tris(2-carboxyethyl)phosphine (TCEP), and thiosemicarbazide were acquired from Sigma−Aldrich. Diacetylmonooxime (DAMO), *N*-α-benzoyl-L-arginine ethyl ester (BAEE), and *N*-α-benzoyl-L-arginine amide (BAA) were obtained from Acros. Detailed synthetic procedures are described in the Supporting Information. PAD1, -2, -3, and -4 were purified analogously to previously described methods.[35,57]

Inactivation Kinetics. The kinetic parameters of inactivation were determined by incubating PAD1, -2, or -4 (2.0 μM) or PAD3 (5.0 μM) in a prewarmed (10 min, 37 °C) inactivation mixture (50 mM HEPES, 10 mM CaCl$_2$, and 2 mM DTT, pH 7.6, with a final volume of 60 μL) containing various concentrations of inhibitor. Aliquots were removed at various time points (0, 2, 6, 10, 15, 20, and 30 min or 0, 0.5, 1, 1.5, 2, 4, and 6 min) and added to a prewarmed (10 min, 37 °C) reaction mixture (50 mM HEPES, 50 mM NaCl, 10 mM CaCl$_2$, 2 mM DTT, and 10 mM BAEE or 10 mM BAA in the case of PAD3; pH 7.6). After 15 min, reactions were quenched in liquid nitrogen and citrulline production quantified using the COLDER assay.[58,59] Data were plotted as a function of time and fit to eq 1,

$$v = v_o\, e^{-k_{obs}t} \qquad (1)$$

using GraFit, version 5.0.11, where v is velocity, v_o is the initial velocity, k_{obs} is the pseudo-first-order rate constant of inactivation (i.e., k_{obs}), and t is time. The k_{obs} values were then plotted against inhibitor concentration, and the data were fit to eq 2,

$$k_{obs} = k_{inact}[I]/(K_I) \qquad (2)$$

using GraFit, version 5.0.11. Since saturation was not observed in any of the plots, k_{inact}/K_I was calculated from the slope of the line. k_{inact} corresponds to the maximal rate of inactivation, and K_I is the concentration of inhibitor that gives half-maximal inactivation. For a subset of the less potent compounds, k_{inact}/K_I values were determined by dividing the k_{obs} value at a single concentration by the concentration of the inhibitor tested.

Cell Viability. The human osteosarcoma (U2OS) cell line was plated (2.5×10^6 cells/well) in a 96-well plate. The next day the cells were treated with compounds (5 μL, 20 μM final), DMSO (5 μL), Triton X-100 (5 μL), or various concentrations of **13** or **14** and incubated for 72 h. Cell viability was measured using the XTT reagent kit (ATCC) by reading the absorption at 475 nm using a Spectramax plate reader. EC_{50} values for cell growth inhibition were determined by fitting an eight-point dose−response curve to eq 3,

$$Y = \frac{range}{1 + \left(\frac{[I]}{EC_{50}}\right)^s} + background \qquad (3)$$

using GraFit5.0.11, where range is the uninhibited value minus the background and s is the slope factor. For in vitro cytotoxicity assays with neutrophils, freshly isolated human neutrophils were resuspended in RPMI 1640 medium containing 10% fetal bovine serum and then seeded into poly-L-lysine coated 96-well plates at 40 000 cells/well. After the cells were allowed to adhere for 1 h, neutrophils were incubated for 4 h with **13** or **21** at concentrations ranging from 1 to 500 μM. Cell viability after drug exposure was measured using the XTT cell viability kit as described above.

Neutrophil Isolation. C57BL/6 mice were purchased from The Jackson Laboratory. Bone marrow neutrophils were isolated essentially as described previously.[60] Briefly, bone marrow was flushed from femurs and tibias with Hank's balanced salt solution supplemented with 15 mM EDTA. Cells were then spun on a discontinuous Percoll gradient (52%, 69%, 78%) at 1500g for 30 min. Cells from the 69−78% interface were collected, and red blood cells were lysed. Cells were >95% Ly-6G-positive and had typical segmented nuclei by microscopy.

NET Quantification and Microscopy. A protocol similar to what we have described previously was followed.[61] Briefly, 1.5×10^5 neutrophils were seeded onto glass coverslips coated with 0.001% poly-L-lysine (Sigma). PAD inhibitors were used at the indicated concentrations, including a 30 min pretreatment in Locke's solution (150 mM NaCl, 5 mM KCl, 2 mM CaCl$_2$, 0.1% glucose, and 10 mM HEPES buffer, pH 7.3). Stimulation was with 100 nM PMA (Sigma) for 3−4 h in RPMI-1640 supplemented with L-glutamine, 2% BSA, and 10 mM HEPES buffer. Cells were then fixed with 4% paraformaldehyde (PFA) for 20 min, followed by blocking with 10% fetal bovine serum; cells were not specifically permeabilized. DNA was stained with Hoechst 33342 (Invitrogen), while protein staining was with a rabbit polyclonal antibody to myeloperoxidase (A0398, Dako) followed by FITC-conjugated anti-rabbit IgG (4052-02, SouthernBiotech). After staining, coverslips were mounted in Prolong Gold antifade reagent (Invitrogen). Images were collected with an Olympus microscope (IX70) and a CoolSNAP HQ2 monochrome camera (Photometrics) with Metamorph Premier software (Molecular Devices), typically at 400× magnification. Statistical background correction and image overlays were with Metamorph, and the recorded images were loaded onto Adobe Photoshop for further analysis, at which time NETs were manually quantified by two blinded observers. Decondensed nuclei that also stained positively for myeloperoxidase were considered NETs and digitally recorded to prevent multiple counts. The percentage of NETs was calculated as the average of at least five fields and normalized to the total number of cells.

ASSOCIATED CONTENT

$\circledS$ Supporting Information

Synthetic procedures, experimental details, and Table S1. This material is available free of charge via the Internet at http://pubs.acs.org.

AUTHOR INFORMATION

Corresponding Author

*Phone: 508-856-8492. Fax: 508-856-6215. E-mail: Paul. Thompson@umassmed.edu.

Notes

The authors declare the following competing financial interest(s): P.R.T is a cofounder and consultant to Padlock Therapeutics.

ABBREVIATIONS USED

TFA, trifluoroacetic acid; MeOH, methanol; ACN, acetonitrile; DMF, dimethylformamide; NMM, *N*-methylmorpholine; HBTU, *O*-benzotriazole-N,N,N′,N′-tetramethyluronium hexafluorophosphate; DTT, dithiothreitol; BAEE, benzoyl-L-arginine ethyl ester; BAA, benzoyl-L-arginine amide; PAD, protein arginine deiminase; COLDER, color development reagent; Bz, benzoyl; Orn, ornithine; T, tetrazole; TT, tetrazole *tert*-butyl; B, biphenyl

REFERENCES

(1) Stone, E. M.; Schaller, T. H.; Bianchi, H.; Person, M. D.; Fast, W. Inactivation of two diverse enzymes in the amidinotransferase superfamily by 2-chloroacetamidine: dimethylargininase and peptidyl-larginine deiminase. *Biochemistry* **2005**, *44*, 13744−13752.

(2) Jones, J. E.; Causey, C. P.; Knuckley, B.; Slack-Noyes, J. L.; Thompson, P. R. Protein arginine deiminase 4 (PAD4): current understanding and future therapeutic potential. *Curr. Opin Drug Discovery Dev.* **2009**, *12*, 616−627.

(3) Vossenaar, E. R.; Zendman, A. J.; van Venrooij, W. J.; Pruijn, G. J. PAD, a growing family of citrullinating enzymes: genes, features and involvement in disease. *BioEssays* **2003**, *25*, 1106−1118.

(4) Slade, D. J.; Subramanian, V.; Thompson, P. R. Citrullination unravels stem cells. *Nat. Chem. Biol.* **2014**, *10*, 327−328.

(5) Slade, D. J.; Subramanian, V.; Fuhrmann, J.; Thompson, P. R. Chemical and biological methods to detect post-translational modifications of arginine. *Biopolymers* **2014**, *101*, 133−143.

(6) Suzuki, A.; Yamada, R.; Yamamoto, K. Citrullination by peptidylarginine deiminase in rheumatoid arthritis. *Ann. N.Y. Acad. Sci.* **2007**, *1108*, 323−339.

(7) Vossenaar, E. R.; Nijenhuis, S.; Helsen, M. M.; van der Heijden, A.; Senshu, T.; van den Berg, W. B.; van Venrooij, W. J.; Joosten, L. A. Citrullination of synovial proteins in murine models of rheumatoid arthritis. *Arthritis Rheum.* **2003**, *48*, 2489−2500.

(8) Moscarello, M. A.; Mastronardi, F. G.; Wood, D. D. The role of citrullinated proteins suggests a novel mechanism in the pathogenesis of multiple sclerosis. *Neurochem. Res.* **2007**, *32*, 251−256.

(9) Ishigami, A.; Ohsawa, T.; Hiratsuka, M.; Taguchi, H.; Kobayashi, S.; Saito, Y.; Murayama, S.; Asaga, H.; Toda, T.; Kimura, N.; Maruyama, N. Abnormal accumulation of citrullinated proteins catalyzed by peptidylarginine deiminase in hippocampal extracts

from patients with Alzheimer's disease. *J. Neurosci. Res.* **2005**, *80*, 120−128.

(10) Jang, B.; Jin, J. K.; Jeon, Y. C.; Cho, H. J.; Ishigami, A.; Choi, K. C.; Carp, R. I.; Maruyama, N.; Kim, Y. S.; Choi, E. K. Involvement of peptidylarginine deiminase-mediated post-translational citrullination in pathogenesis of sporadic Creutzfeldt−Jakob disease. *Acta Neuropathol.* **2010**, *119*, 199−210.

(11) Jang, B.; Kim, E.; Choi, J. K.; Jin, J. K.; Kim, J. I.; Ishigami, A.; Maruyama, N.; Carp, R. I.; Kim, Y. S.; Choi, E. K. Accumulation of citrullinated proteins by up-regulated peptidylarginine deiminase 2 in brains of scrapie-infected mice: a possible role in pathogenesis. *Am. J. Pathol.* **2008**, *173*, 1129−1142.

(12) Wang, Y.; Li, P.; Wang, S.; Hu, J.; Chen, X. A.; Wu, J.; Fisher, M.; Oshaben, K.; Zhao, N.; Gu, Y.; Wang, D.; Chen, G.; Wang, Y. Anticancer peptidylarginine deiminase (PAD) inhibitors regulate the autophagy flux and the mammalian target of rapamycin complex 1 activity. *J. Biol. Chem.* **2012**, *287*, 25941−25953.

(13) Harauz, G.; Musse, A. A. A tale of two citrullines—structural and functional aspects of myelin basic protein deimination in health and disease. *Neurochem. Res.* **2007**, *32*, 137−158.

(14) Kidd, B. A.; Ho, P. P.; Sharpe, O.; Zhao, X.; Tomooka, B. H.; Kanter, J. L.; Steinman, L.; Robinson, W. H. Epitope spreading to citrullinated antigens in mouse models of autoimmune arthritis and demyelination. *Arthritis Res. Ther.* **2008**, *10*, R119.

(15) Rohrbach, A. S.; Slade, D. J.; Thompson, P. R.; Mowen, K. A. Activation of PAD4 in NET formation. *Front. Immunol.* **2012**, *3*, 360.

(16) Li, P.; Li, M.; Lindberg, M. R.; Kennett, M. J.; Xiong, N.; Wang, Y. PAD4 is essential for antibacterial innate immunity mediated by neutrophil extracellular traps. *J. Exp. Med.* **2010**, *207*, 1853−1862.

(17) Luo, Y.; Knuckley, B.; Lee, Y. H.; Stallcup, M. R.; Thompson, P. R. A fluoroacetamidine-based inactivator of protein arginine deiminase 4: design, synthesis, and in vitro and in vivo evaluation. *J. Am. Chem. Soc.* **2006**, *128*, 1092−1093.

(18) Luo, Y.; Arita, K.; Bhatia, M.; Knuckley, B.; Lee, Y. H.; Stallcup, M. R.; Sato, M.; Thompson, P. R. Inhibitors and inactivators of protein arginine deiminase 4: functional and structural characterization. *Biochemistry* **2006**, *45*, 11727−11736.

(19) Knuckley, B.; Luo, Y.; Thompson, P. R. Profiling protein arginine deiminase 4 (PAD4): a novel screen to identify PAD4 inhibitors. *Bioorg. Med. Chem.* **2008**, *16*, 739−745.

(20) Golub, L. M.; McNamara, T. F.; D'Angelo, G.; Greenwald, R. A.; Ramamurthy, N. S. A non-antibacterial chemically-modified tetracycline inhibits mammalian collagenase activity. *J. Dent. Res.* **1987**, *66*, 1310−1314.

(21) Greenwald, R. A.; Golub, L. M.; Lavietes, B.; Ramamurthy, N. S.; Gruber, B.; Laskin, R. S.; McNamara, T. F. Tetracyclines inhibit human synovial collagenase in vivo and in vitro. *J. Rheumatol.* **1987**, *14*, 28−32.

(22) Golub, L. M.; Lee, H. M.; Lehrer, G.; Nemiroff, A.; McNamara, T. F.; Kaplan, R.; Ramamurthy, N. S. Minocycline reduces gingival collagenolytic activity during diabetes. Preliminary observations and a proposed new mechanism of action. *J. Periodontal Res.* **1983**, *18*, 516−526.

(23) Alano, C. C.; Kauppinen, T. M.; Valls, A. V.; Swanson, R. A. Minocycline inhibits poly(ADP-ribose) polymerase-1 at nanomolar concentrations. *Proc. Natl. Acad. Sci. U.S.A.* **2006**, *103*, 9685−9690.

(24) Imamura, T.; Matsushita, K.; Travis, J.; Potempa, J. Inhibition of trypsin-like cysteine proteinases (gingipains) from *Porphyromonas gingivalis* by tetracycline and its analogues. *Antimicrob. Agents Chemother.* **2001**, *45*, 2871−2876.

(25) Pruzanski, W.; Vadas, P. Should tetracyclines be used in arthritis? *J. Rheumatol.* **1992**, *19*, 1495−1497.

(26) Trentham, D. E.; Dynesius-Trentham, R. A. Antibiotic therapy for rheumatoid arthritis. Scientific and anecdotal appraisals. *Rheum. Dis. Clin. North Am.* **1995**, *21*, 817−834.

(27) Forsgren, A.; Schmeling, D.; Quie, P. G. Effect of tetracycline on the phagocytic function of human leukocytes. *J. Infect. Dis.* **1974**, *130*, 412−415.

(28) Li, P.; Yao, H.; Zhang, Z.; Li, M.; Luo, Y.; Thompson, P. R.; Gilmour, D. S.; Wang, Y. Regulation of p53 target gene expression by peptidylarginine deiminase 4. *Mol. Cell. Biol.* **2008**, *28*, 4745−4758.

(29) Zhang, X.; Bolt, M.; Guertin, M. J.; Chen, W.; Zhang, S.; Cherrington, B. D.; Slade, D. J.; Dreyton, C. J.; Subramanian, V.; Bicker, K. L.; Thompson, P. R.; Mancini, M. A.; Lis, J. T.; Coonrod, S. A. Peptidylarginine deiminase 2-catalyzed histone H3 arginine 26 citrullination facilitates estrogen receptor alpha target gene activation. *Proc. Natl. Acad. Sci. U.S.A.* **2012**, *109*, 13331−13336.

(30) Zhang, X.; Gamble, M. J.; Stadler, S.; Cherrington, B. D.; Causey, C. P.; Thompson, P. R.; Roberson, M. S.; Kraus, W. L.; Coonrod, S. A. Genome-wide analysis reveals PADI4 cooperates with Elk-1 to activate c-Fos expression in breast cancer cells. *PLoS Genet.* **2011**, *7*, e1002112.

(31) Yao, H.; Li, P.; Venters, B. J.; Zheng, S.; Thompson, P. R.; Pugh, B. F.; Wang, Y. Histone Arg modifications and p53 regulate the expression of OKL38, a mediator of apoptosis. *J. Biol. Chem.* **2008**, *283*, 20060−20068.

(32) Wang, Y.; Li, M.; Stadler, S.; Correll, S.; Li, P.; Wang, D.; Hayama, R.; Leonelli, L.; Han, H.; Grigoryev, S. A.; Allis, C. D.; Coonrod, S. A. Histone hypercitrullination mediates chromatin decondensation and neutrophil extracellular trap formation. *J. Cell Biol.* **2009**, *184*, 205−213.

(33) Chumanevich, A. A.; Causey, C. P.; Knuckley, B. A.; Jones, J. E.; Poudyal, D.; Chumanevich, A. P.; Davis, T.; Matesic, L. E.; Thompson, P. R.; Hofseth, L. J. Suppression of colitis in mice by Cl-amidine: a novel peptidylarginine deiminase inhibitor. *Am. J. Physiol.: Gastrointest. Liver Physiol.* **2011**, *300*, G929−938.

(34) Lange, S.; Gogel, S.; Leung, K. Y.; Vernay, B.; Nicholas, A. P.; Causey, C. P.; Thompson, P. R.; Greene, N. D.; Ferretti, P. Protein deiminases: new players in the developmentally regulated loss of neural regenerative ability. *Dev. Biol.* **2011**, *355*, 205−214.

(35) Causey, C. P.; Jones, J. E., Jr.; Slack, J. L.; Kamei, D.; Jones, L. E.; Subramanian, V.; Knuckley, B.; Ebrahimi, P.; Chumanevich, A. A.; Luo, Y.; Hashimoto, H.; Sato, M.; Hofseth, L. J.; Thompson, P. R. The development of *N*-α-(2-carboxyl)benzoyl-*N*⁵-(2-fluoro-1-iminoethyl)-L-ornithine amide (*o*-F-amidine) and *N*-α-(2-carboxyl)benzoyl-*N*⁵-(2-chloro-1-iminoethyl)-L-ornithine amide (*o*-Cl-amidine) as second generation protein arginine deiminase (PAD) inhibitors. *J. Med. Chem.* **2011**, *54*, 6919−6935.

(36) Knight, J. S.; Kaplan, M. J. Lupus neutrophils: "NET" gain in understanding lupus pathogenesis. *Curr. Opin. Rheumatol.* **2012**, *24*, 441−450.

(37) Knight, J. S.; Zhao, W.; Luo, W.; Subramanian, V.; O'Dell, A. A.; Yalavarthi, S.; Hodgin, J. B.; Eitzman, D. T.; Thompson, P. R.; Kaplan, M. J. Peptidylarginine deiminase inhibition is immunomodulatory and vasculoprotective in murine lupus. *J. Clin. Invest.* **2013**, *123*, 2981−2993.

(38) Khandpur, R.; Carmona-Rivera, C.; Vivekanandan-Giri, A.; Gizinski, A.; Yalavarthi, S.; Knight, J. S.; Friday, S.; Li, S.; Patel, R. M.; Subramanian, V.; Thompson, P.; Chen, P.; Fox, D. A.; Pennathur, S.; Kaplan, M. J. NETs are a source of citrullinated autoantigens and stimulate inflammatory responses in rheumatoid arthritis. *Sci. Transl. Med.* **2013**, *5*, 178ra140.

(39) Smith, C. K.; Vivekanandan-Giri, A.; Tang, C.; Knight, J. S.; Mathew, A.; Padilla, R. L.; Gillespie, B. W.; Carmona-Rivera, C.; Liu, X.; Subramanian, V.; Hasni, S.; Thompson, P. R.; Heinecke, J. W.; Saran, R.; Pennathur, S.; Kaplan, M. J. Neutrophil extracellular trap-derived enzymes oxidize high-density lipoprotein: An additional proatherogenic mechanism in systemic lupus erythematosus. *Arthritis Rheum.* **2014**, *66*, 2532−2544.

(40) Knight, J. S.; Luo, W.; O'Dell, A. A.; Yalavarthi, S.; Zhao, W.; Subramanian, V.; Guo, C.; Grenn, R. C.; Thompson, P. R.; Eitzman, D. T.; Kaplan, M. J. Peptidylarginine deiminase inhibition reduces vascular damage and modulates innate immune responses in murine models of atherosclerosis. *Circ. Res.* **2014**, *114*, 947−956.

(41) McElwee, J. L.; Mohanan, S.; Griffith, O. L.; Breuer, H. C.; Anguish, L. J.; Cherrington, B. D.; Palmer, A. M.; Howe, L. R.; Subramanian, V.; Causey, C. P.; Thompson, P. R.; Gray, J. W.;

Coonrod, S. A. Identification of PADI2 as a potential breast cancer biomarker and therapeutic target. *BMC Cancer* **2012**, *12*, 500.

(42) Jones, J. E.; Slack, J. L.; Fang, P.; Zhang, X.; Subramanian, V.; Causey, C. P.; Coonrod, S. A.; Guo, M.; Thompson, P. R. Synthesis and screening of a haloacetamidine containing library to identify PAD4 selective inhibitors. *ACS Chem. Biol.* **2012**, *7*, 160−165.

(43) Bicker, K. L.; Anguish, L.; Chumanevich, A. A.; Cameron, M. D.; Cui, X.; Witalison, E.; Subramanian, V.; Zhang, X.; Chumanevich, A. P.; Hofseth, L. J.; Coonrod, S. A.; Thompson, P. R. D-Amino acid based protein arginine deiminase inhibitors: synthesis, pharmacokinetics, and in cellulo efficacy. *ACS Med. Chem. Lett.* **2012**, *3*, 1081−1085.

(44) Herr, R. J. 5-Substituted-1*H*-tetrazoles as carboxylic acid isosteres: medicinal chemistry and synthetic methods. *Bioorg. Med. Chem.* **2002**, *10*, 3379−3393.

(45) Nachman, R. J.; Zabrocki, J.; Olczak, J.; Williams, H. J.; Moyna, G.; Ian Scott, A.; Coast, G. M. Cis-peptide bond mimetic tetrazole analogs of the insect kinins identify the active conformation. *Peptides* **2002**, *23*, 709−716.

(46) Zabrocki, J.; Marshall, G. R. The 1,5-disubstituted tetrazole ring as a cis-amide bond surrogate. *Methods Mol. Med.* **1999**, *23*, 417−436.

(47) Ostrovskii, V. A.; Koren, A. O. Alkylation and related electrophilic reactions at endocyclic nitrogen atoms in the chemistry of tetrazoles. *Heterocycles* **2000**, *53*, 1421−1448.

(48) Causey, C. P.; Thompson, P. R. An improved synthesis of haloacetamidine-based inactivators of protein arginine deiminase 4 (PAD4). *Tetrahedron Lett.* **2008**, *49*, 4383−4385.

(49) Luo, Y.; Knuckley, B.; Bhatia, M.; Thompson, P. R. Activity based protein profiling reagents for protein arginine deiminase 4 (PAD4): synthesis and in vitro evaluation of a fluorescently-labeled probe. *J. Am. Chem. Soc.* **2006**, *128*, 14468−14469.

(50) Slack, J. L.; Causey, C. P.; Luo, Y.; Thompson, P. R. The development and use of clickable activity based protein profiling agents for protein arginine deiminase 4. *ACS Chem. Biol.* **2011**, *6*, 466−476.

(51) Baranczewski, P.; Stanczak, A.; Sundberg, K.; Svensson, R.; Wallin, A.; Jansson, J.; Garberg, P.; Postlind, H. Introduction to in vitro estimation of metabolic stability and drug interactions of new chemical entities in drug discovery and development. *Pharmacol. Rep.* **2006**, *58*, 453−472.

(52) Leshner, M.; Wang, S.; Lewis, C.; Zheng, H.; Chen, X. A.; Santy, L.; Wang, Y. PAD4 mediated histone hypercitrullination induces heterochromatin decondensation and chromatin unfolding to form neutrophil extracellular trap-like structures. *Front. Immunol.* **2012**, *3*, 307.

(53) Li, P. X.; Li, M.; Lindberg, M. R.; Kennett, M. J.; Xiong, N.; Wang, Y. M. PAD4 is essential for antibacterial innate immunity mediated by neutrophil extracellular traps. *J. Exp. Med.* **2010**, *207*, 1853−1862.

(54) Martinod, K.; Demers, M.; Fuchs, T. A.; Wong, S. L.; Brill, A.; Gallant, M.; Hu, J.; Wang, Y. M.; Wagner, D. D. Neutrophil histone modification by peptidylarginine deiminase 4 is critical for deep vein thrombosis in mice. *Proc. Natl. Acad. Sci. U.S.A.* **2013**, *110*, 8674−8679.

(55) Brinkmann, V.; Reichard, U.; Goosmann, C.; Fauler, B.; Uhlemann, Y.; Weiss, D. S.; Weinrauch, Y.; Zychlinsky, A. Neutrophil extracellular traps kill bacteria. *Science* **2004**, *303*, 1532−1535.

(56) Brinkmann, V.; Zychlinsky, A. Neutrophil extracellular traps: Is immunity the second function of chromatin? *J. Cell Biol.* **2012**, *198*, 773−783.

(57) Knuckley, B.; Causey, C. P.; Jones, J. E.; Bhatia, M.; Dreyton, C. J.; Osborne, T. C.; Takahara, H.; Thompson, P. R. Substrate specificity and kinetic studies of PADs 1, 3, and 4 identify potent and selective inhibitors of protein arginine deiminase 3. *Biochemistry* **2010**, *49*, 4852−4863.

(58) Knipp, M.; Vasak, M. A colorimetric 96-well microtiter plate assay for the determination of enzymatically formed citrulline. *Anal. Biochem.* **2000**, *286*, 257−264.

(59) Kearney, P. L.; Bhatia, M.; Jones, N. G.; Luo, Y.; Glascock, M. C.; Catchings, K. L.; Yamada, M.; Thompson, P. R. Kinetic characterization of protein arginine deiminase 4: a transcriptional corepressor implicated in the onset and progression of rheumatoid arthritis. *Biochemistry* **2005**, *44*, 10570−10582.

(60) Boxio, R.; Bossenmeyer-Pourie, C.; Steinckwich, N.; Dournon, C.; Nusse, O. Mouse bone marrow contains large numbers of functionally competent neutrophils. *J. Leukocyte Biol.* **2004**, *75*, 604−611.

(61) Villanueva, E.; Yalavarthi, S.; Berthier, C. C.; Hodgin, J. B.; Khandpur, R.; Lin, A. M.; Rubin, C. J.; Zhao, W. P.; Olsen, S. H.; Klinker, M.; Shealy, D.; Denny, M. F.; Plumas, J.; Chaperot, L.; Kretzler, M.; Bruce, A. T.; Kaplan, M. J. Netting neutrophils induce endothelial damage, infiltrate tissues, and expose immunostimulatory molecules in systemic lupus erythematosus. *J. Immunol.* **2011**, *187*, 538−552.